

# Electrochemical oxidation of butyl paraben on boron doped diamond in environmental matrices and comparison with sulfate radical-AOP

Noelia Pueyo<sup>a</sup>, Maria P. Ormad<sup>a</sup>, Natividad Miguel<sup>a</sup>, Petros Kokkinos<sup>b</sup>,  
Alexandra Ioannidi<sup>b</sup>, Dionissios Mantzavinos<sup>b\*</sup>, Zacharias Frontistis<sup>c</sup>

<sup>a</sup> Department of Chemical Engineering & Environmental Technologies, University of Zaragoza, C/María de Luna 3, Zaragoza, 50018, Spain

<sup>b</sup> Department of Chemical Engineering, University of Patras, Caratheodory 1, University Campus, GR-26504 Patras, Greece

<sup>c</sup> Department of Chemical Engineering, University of Western Macedonia, GR-50132 Kozani, Greece

\* Corresponding author:

Email: mantzavinos@chemeng.upatras.gr; Tel.: +302610996136

## Abstract

The electrochemical oxidation (EO) of butyl paraben (BP) over boron-doped diamond (BDD) anode was studied in this work. Emphasis was put on degradation performance in various actual water matrices, including secondary treated wastewater (WW), bottled water (BW), surface water (SW), ultrapure water (UW), and ultrapure water spiked with humic acid (HA). Experiments were performed utilizing 0.1 M Na<sub>2</sub>SO<sub>4</sub> as the electrolyte. Interestingly, matrix complexity was found to favor BP degradation, i.e. in the order WW~BW>SW>UW, thus implying some kind of synergy between the water matrix constituents, the reactive oxygen species (ROS) and the anode surface. The occurrence of chloride in water matrices favors reaction presumably due to the formation of chlorine-based oxidative species, and this can partially offset the need to work at increased current densities in the case of chlorine-free electrolytes. No pH effect in the range 3-8 on degradation was recorded. EO oxidation was also compared with a sulfate radical process using carbon black as activator of sodium persulfate. The matrix effect was, in this case, detrimental (i.e. UW>BW>WW), pinpointing the different behavior of different processes in similar environments.

*Keywords:* aqueous matrix; anodic oxidation; carbocatalysis; electrolytes; emerging contaminants; persulfate

## 1. Introduction

35 Advanced oxidation processes (AOPs, e.g. heterogeneous and homogeneous photocatalysis,  
36 electrochemical oxidation (EO), ozonation, ultrasound irradiation, Fenton and alike reactions,  
37 amongst others) have been investigated for the removal of emerging organic pollutants during the  
38 last decades (Klavarioti et al., 2009). Micropollutants' removal from water matrices has been  
39 recognized as an important environmental and health issue. Water matrix may exert influence on  
40 the electrochemical treatment on boron-doped diamond (BDD) anode. This is due to the high  
41 concentrations of numerous interfering organic and inorganic species, which are usually present in  
42 real effluent samples (Tsantaki et al., 2012). So far, the majority of studies concerning the  
43 application of AOPs for water/wastewater treatment have been performed (and still are) in ultrapure  
44 water. The rationale behind this is associated with the need to obtain basic knowledge with respect  
45 to the degradation kinetics, mechanisms and pathways excluding the water matrix effect.  
46 Nonetheless, the effect itself may be unpredictably important, thus leading to erroneous  
47 conclusions. In most cases, treatment efficiency decreases with increasing water matrix complexity.  
48 This is due to the fact that the target pollutant is likely to compete with the non-target constituents  
49 of the matrix (e.g. organics, inorganics and microorganisms) for the precious oxidant species, as  
50 well as (in the case of heterogeneous processes) for the active sites of the catalysts/activators  
51 (Frontistis and Mantzavinos, 2017). In the study of Kenova et al. (2018), on the electrooxidation of  
52 Mordant Blue 13 azo dye in different water matrices, both electrode material and water matrix  
53 parameters have been reported to significantly affect COD removal and dye decolorization.

54 Electrochemical oxidation has emerged as an environmentally clean technology and BDD has been  
55 shown to be one of the most auspicious anodes for environmental applications (Frontistis et al.,  
56 2017; Sarkka et al., 2015). BDD anodes are known to enhance the generation of ROS compared to  
57 other anodic materials (Pecková et al., 2009); this facilitates the effective conversion of organic  
58 micropollutants of emerging concern and, subsequently, their mineralization. However, the exact  
59 mechanisms of  $O_2$  and  $\cdot OH$  production have not been completely elucidated (Henke et al., 2019;  
60 Kraft et al., 2003).

61 Sulfate radical oxidation processes (SR-AOPs) have recently been developed for water treatment.  
62 Sulfate radicals can be produced after activation of compounds belonging to the group of  
63 persulfates. Activation can occur via numerous methods including, amongst others, heat, transition  
64 metals, light irradiation and ultrasound irradiation (Matzek and Carter, 2016). In recent years,  
65 metal-free carbonaceous materials have been proposed as alternative catalytic materials for  
66 environmental applications (Abid et al., 2016), including persulfate activation. Activated carbon,  
67 graphene, multi-walled carbon nanotubes and biochars are some characteristic examples. Carbon  
68 black (CB), mainly consisting of fine particles of carbon, has recently been proposed as a low-cost

69 alternative to expensive carbon materials, such as graphene, in the field of electrochemistry  
70 showing great performance as an electric conductive agent (Lounasvuori et al., 2018).

71 Parabens are synthetic chemicals used as preservatives in a wide variety of products, like  
72 pharmaceuticals, cosmetics and food. Parabens are excreted through urine as 4-hydroxybenzoic acid  
73 (Fransway et al., 2019b), and are considered contaminants of emerging concern (Frontistis et al.,  
74 2017). In medications, they are recommended at concentrations of no more than 0.1%, and they are  
75 allowed as preservatives in cosmetics at concentrations up to 0.4% when used alone (in the United  
76 States). The acceptable daily intake (ADI) has been calculated to be 10 mg/kg of body weight  
77 (Fransway et al., 2019a, 2019b; Reeder and Atwater, 2019; Liao et al., 2013).

78 Concerns exist regarding the endocrine disruption or carcinogenicity associated with parabens.  
79 However, it should be noted that controversial results have been reported for their health effects  
80 (Reeder and Atwater, 2019; Haman et al., 2015). Since parabens are ubiquitous in environmental  
81 matrices worldwide, efficient treatment processes must be employed for their elimination and to  
82 avert their accumulation (Haman et al., 2015).

83 Few articles exist on parabens treatment by advanced oxidation processes, and specifically by  
84 electrochemical methods (Gomes et al., 2016), and even less dealing with BDD oxidation  
85 (Frontistis et al., 2017; Dominguez et al., 2016; Steter et al., 2014a; 2014b). It should be noted that  
86 the studies of Steter et al. (2014a; 2014b) focus on the elimination and mineralization of an  
87 unrealistically high concentration of methyl paraben for environmental samples (100 mg/L). Much  
88 lower parabens concentrations (in the range of  $\mu\text{g/L}$ ) have been measured in influent of domestic  
89 wastewater treatment plants (WTP) (Giger et al., 2009). Dominguez et al. (2016) examined  
90 parabens decomposition efficiency by BDD oxidation in aqueous matrices and found that the initial  
91 concentration was the most important factor. Notably, an increase of the initial paraben  
92 concentration caused a decrease of the efficiency of their removal. Interestingly, a synergistic effect  
93 on the efficiency of removal has been recorded in surface water (river). This finding was attributed  
94 to the probable presence of chloride ions, the resulting rise of solution conductivity and the  
95 formation of additional secondary oxidant species that diffuse in the bulk solution (Dominguez et  
96 al., 2016).

97 In one of our previous studies (Frontistis et al., 2017) regarding the BDD mediated oxidation of  
98 ethyl paraben at environmentally rational concentration (at the  $\mu\text{g/L}$  concentration level), we found  
99 that the removal rate followed a pseudo-first order kinetic expression concerning paraben  
100 concentration and depended on the type of supporting electrolyte, the current density, and the  
101 complexity of the water matrix. In the context of the same study, reaction mechanisms were  
102 postulated by identifying major transformation by-products and elucidating reaction pathways with  
103 different electrolytes.

104 In the present study, we further focused on the water matrix effect on the BDD anodic oxidation for  
105 the degradation of BP at a concentration level of 0.5 mg/L, by studying various water matrices,  
106 including bottled water, secondary effluent, surface water, ultrapure water and ultrapure water  
107 spiked with humic acid. Moreover, anodic oxidation was compared to SR-AOP concerning process  
108 efficiency in actual matrices to highlight how possible interferences amongst target and non-target  
109 water constituents may dictate treatment performance.

110

## 111 **2. Experimental and analytical**

### 112 2.1. Chemicals

113 Butyl paraben (BP) ( $\text{HO-C}_6\text{H}_4\text{-CO-O-(CH}_2\text{)}_3\text{-CH}_3$ , CAS no: 94-26-8) was provided by Sigma-  
114 Aldrich. Solutions were prepared by using ultrapure water (UW, pH=6.5) which was derived from a  
115 Millipore Milli-Q Gradient A10 system. To test the effect of matrix, various actual water matrices,  
116 including WW, BW, SW, UW, and UW spiked with HA were used. For experiments with BW, a  
117 commercially available natural mineral water was used. WW was sampled from the WTP of the  
118 University of Patras, while SW was collected from the region of Attica, Greece (TOC = 2.7 mg/L,  
119 pH = 7.5). More details on BW, WW and SW characteristics are given elsewhere (Frontistis et al.,  
120 2017; Tsiampalis et al., 2019). Technical grade humic acid (HA, CAS no: 1415-93-6) was supplied  
121 from Sigma-Aldrich. Sulfuric acid or sodium hydroxide used for pH adjustment, sodium chloride,  
122 sodium sulfate, sodium bicarbonate, sodium persulfate (SPS:  $\text{Na}_2\text{S}_2\text{O}_8$ ), methanol and t-butanol  
123 were purchased from Sigma-Aldrich. Carbon black (CB: Vulcan XC72R) was supplied by Cabot.

124

### 125 2.2. Reactor setup and experimental procedure

126 The experimental set up of the electrochemical reactor consisted of two electrodes (a boron doped  
127 diamond electrode served as the anode and a 304 stainless steel electrode served as the cathode,  
128 both with a surface area of  $8 \text{ cm}^2$ ). More information can be found in other studies of our group  
129 (Kouskouki et al., 2018; Frontistis et al., 2017). In specific experiments, stainless steel and  
130 platinum with a surface area of  $8 \text{ cm}^2$  were also used as anode to examine the effect of the anodic  
131 material.

132 In order to evaluate the influence of operating conditions on BP removal, experiments were  
133 conducted at  $1.4\text{-}143 \text{ mA/cm}^2$  current density, 0.1 M electrolyte concentration and  $250\text{-}2000 \text{ }\mu\text{g/L}$   
134 BP concentration. Experiments were performed at their inherent pH, except of the experiments that  
135 were conducted at acidic or alkaline conditions with the addition of the appropriate volume of  
136  $\text{H}_2\text{SO}_4$  or NaOH.

137 For SR-AOP experiments, a pyrex vessel of 250 mL capacity open to the atmosphere was  
138 employed. In a typical run, 120 mL of an aqueous solution containing 0.5 mg/L BP was loaded in

139 the vessel followed by the addition of CB and SPS. The solution was under continuous magnetic  
140 stirring.

141 From either reactor, samples of 1.2 mL were collected at specific times, filtered with a 0.22  $\mu\text{m}$   
142 syringe filter (PVDF) and then measured as follows.

143

### 144 2.3 Determination of BP

145 High performance liquid chromatography (Waters Alliance 2695) interfaced with a photodiode  
146 array detector (Waters 2996) was used for the detection of BP. Separation was achieved on a  
147 Kinetex XB-C18 100A column (2.6  $\mu\text{m}$ , 2.1 mm x 150 mm) and a 0.5  $\mu\text{m}$  inline filter (KrudKatcher  
148 Ultra) both purchased from Phenomenex. The mobile phase, consisting of 50:50 UW:acetonitrile,  
149 eluted isocratically at 0.25 mL/min and 45°C, while the injection volume was 100  $\mu\text{L}$ .

150

## 151 3. Results and discussion

### 152 3.1. Effect of operating conditions on degradation

#### 153 3.1.1. Effect of the anodic material

154 Wide variations exist between different electrode materials as it concerns their efficiency to oxidize  
155 water to  $\bullet\text{OH}$  or  $\text{O}_2$ , and the nature of adsorbed radicals/electrode surface interaction.

156 In the present study, preliminary experiments were performed to investigate the effect of anodic  
157 material (BDD, stainless steel, platinum) on the degradation of 0.5 mg/L BP at 50 mA/cm<sup>2</sup> current  
158 density with 0.1 M Na<sub>2</sub>SO<sub>4</sub> in UW and the results are presented in Figure 1. As can be seen,  
159 complete destruction of BP was achieved in 15 min of treatment with BDD anode, while the  
160 removal was about 40% and 18% for steel or platinum anode, respectively. BP removal was solely  
161 due to electrochemical processes and not just adsorption on the BDD surface as preliminary  
162 equilibration experiments had shown.

163 The results are in agreement with the work of Kouskouki et al. (2019), who observed complete  
164 removal of 245  $\mu\text{g/L}$  piroxicam at 26.7 mA/cm<sup>2</sup> on BDD after 15 min of electrooxidation, while  
165 only 15% removal occurred in the presence of platinum.

166 The better efficiency of BDD anodic material compared to that of steel or platinum, may be  
167 attributed to the larger production of  $\bullet\text{OH}$  on its surface. BDD is classified as “non-active”  
168 electrode, thus the surface of the BDD has only a physical interaction with  $\bullet\text{OH}$  and, consequently,  
169 a greater production of hydroxyl radicals without forming higher oxides (Muruganathan et al.,  
170 2008). Likewise, a much better efficiency of BDD in comparison to RuO<sub>2</sub>, glassy carbon, Pt, and  
171 PbO<sub>2</sub>, anodes has been described by Burgos-Castillo et al. (2018) and Muruganathan et al. (2008).  
172 Frontistis et al. (2018) reported that BDD was found to be more effective than platinum, since  
173 ampicillin abatement after 10 min of electrolysis was 39% and 68% for platinum and BDD,

174 respectively. Similarly, BDD was found to have a significantly higher efficiency compared to  
175 platinum for the EO and mineralization of salicylic acid (Guinea et al., 2008). In the study of  
176 Barazesh et al. (2016), degradation rates normalized per surface area of BDD anode were several  
177 times (i.e. 100–2500%) greater than in Ti–IrO<sub>2</sub>.

178 BDD is considered as an ideal anodic material due to outstanding chemical, physical and  
179 electrochemical properties compared to other conventional electrode materials. The results of the  
180 present study confirm this finding, further supporting the technology of EO over BDD anodes  
181 which holds great promise to provide efficient wastewater treatment solutions.

182

### 183 *3.1.2. Effect of applied current*

184 Since electrons represent the energy input of the system, the role of the applied current is vital. The  
185 increase in current density favors the formation of •OH, which in turn may maximize the  
186 mineralization of organic pollutants. Figure 2 shows the effect of applied current density on 0.5  
187 mg/L BP degradation in UW with 0.1 M Na<sub>2</sub>SO<sub>4</sub>. As seen in Figure 2A, which shows  
188 concentration-time profiles, an increase in current density results in increased conversion. Complete  
189 oxidation of BP can be accomplished within 5 min at 107–143 mA/cm<sup>2</sup>, 10 min at 71 mA/cm<sup>2</sup>, and  
190 15 min at 50 mA/cm<sup>2</sup>. Figure 2B shows the effect of current density on the apparent rate constant,  
191  $k_{app}$ , assuming that the electrochemical decomposition of BP follows pseudo-first order kinetics.  
192 Apparent rate constants are calculated from the slope of the straight lines associated with the plot of  
193 the logarithm of normalized concentrations over time (plots are not shown for brevity). Frontistis et  
194 al. (2018) showed that the rate of the degradation of antibiotic ampicillin remarkably increased by  
195 increasing current density. Similarly, a three-fold increase in the oxidation rate of ethyl paraben  
196 over BDD was recorded when the current augmented from 10 to 70 mA/cm<sup>2</sup> (Frontistis et al.,  
197 2017). Dominguez et al. (2016) showed that current density affected BDD oxidation of parabens in  
198 a statistically significant manner, in both UW and river water; in other studies (Dominguez et al.,  
199 2010), the influence of current on carbamazepine degradation over BDD was found to be the single  
200 most important variable followed by the concentration of salt and the flow rate. Abdelhay et al.  
201 (2017) showed that increasing applied current density positively affected the removal of color,  
202 COD, and turbidity of slaughterhouse wastewater. In the study of Deligiorgis et al. (2008), on BDD  
203 electrolysis of table olive processing wastewater, a statistically significant effect of the current, the  
204 initial COD, and the contact time on the degradation of phenols and COD was recorded. In another  
205 study, Muruganathan et al. (2008) found that bisphenol A (BPA) oxidation was a current-  
206 controlled process and occurred faster at greater current densities. In the study of Kenova et al.  
207 (2018), the decolorization of Mordant Blue 13 dye followed exponential decay with  $k_{app}$  increasing  
208 with increasing applied current density. According to the authors, a remarkable increase in the dye

209 removal rate at higher current density was due to the formation of additional radicals and other  
210 oxidizing species, (e.g. sulfate radicals, peroxodisulfate anions,  $H_2O_2$ ). The removal of COD was  
211 increased with specific charge. However, the variation of current density had almost no effect on  
212 COD removal. This finding suggests the crucial role of mediated oxidation in the electrochemical  
213 oxidation. Interestingly, the work of Anglada et al. (2011) on the BDD electrolysis of landfill  
214 leachate showed that no statistically significant effect of the applied current on the removal of the  
215 pollutants was noted, under the studied conditions.

216

### 217 *3.1.3. Effect of BP concentration*

218 Figure 3 shows the influence of BP concentration on its degradation at  $50 \text{ mA/cm}^2$  current density  
219 in UW with  $0.1 \text{ M Na}_2\text{SO}_4$ . Increasing initial concentration decreases the rate, which implies that  
220 the concentration of oxidants generated during the process is a limiting factor for the decomposition  
221 of organics. In fact, the rate that the oxidants are produced is expected to be nearly constant at fixed  
222 operating conditions, i.e. current density and the electrolyte used. Thus, the rate BP is degraded is a  
223 function of its concentration relative to the oxidants available for reaction and it decreases at higher  
224 BP concentrations. It should be noted here that although degradation data can still be fitted  
225 adequately to a pseudo-first order kinetic model from which  $k_{app}$  values are computed (shown next  
226 to the respective profiles in Figure 3), it is clear that the reaction is not true first order since rate  
227 constants change with initial BP concentration. In fact, this behavior implies a transition of rate  
228 order in regards to BP from first to zeroth.

229 Dominguez et al. (2016) showed that the initial parabens concentration was the unique most  
230 influential factor for their electrochemical removal in ultrapure water and river water; an increase in  
231 the organics concentration resulted in a decline in the efficiency. Frontistis et al. (2018) found that  
232 nearly complete degradation of ampicillin could be reached after 20 min of treatment,  
233 independently of the initial concentration in the range  $0.8\text{-}3 \text{ mg/L}$ . Moreover, the percent removal  
234 was higher for lower concentration of ampicillin. This finding indicates that ampicillin removal did  
235 not follow true first order kinetics with regards to the concentration of ampicillin. In another study  
236 of Muruganathan et al. (2008), it was shown that BPA concentration could affect its mineralization,  
237 especially at the early stages of the reaction. An increase of the mineralization current efficiency  
238 (which is a measure of energy consumption) was recorded with increasing pollutant concentration,  
239 and decreasing current density (Muruganathan et al., 2008).

240

### 241 *3.1.4. Effect of water matrices*

242 Since electrochemical oxidation aims at treating real wastewater, the efficiency of the method in  
243 real aqueous matrices and not only in synthetic wastes is of particular interest. Figure 4A shows the

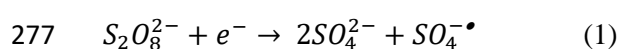
244 effect of various actual water matrices, including WW containing ca 10 mg/L organic carbon and  
 245 inorganics, BW containing mainly ca 250 mg/L bicarbonate, SW, UW, and UW spiked with 10  
 246 mg/L HA (i.e. to simulate the natural organic matter of waters), on the degradation of 0.5 mg/L BP  
 247 at 50 mA/cm<sup>2</sup> current density with 0.1 M Na<sub>2</sub>SO<sub>4</sub>. Interestingly, matrix complexity seems to favor  
 248 BP degradation, i.e. the rate decreases in the order WW~BW>SW>UW, thus implying some kind  
 249 of synergy between the organic and/or inorganic water matrix constituents, ROS and the anode  
 250 surface. The findings of the present study are in agreement with previous studies of our group  
 251 (Frontistis et al., 2017), where the researchers examined the BDD electrooxidation of 200 µg/L  
 252 ethyl paraben in 0.1 M Na<sub>2</sub>SO<sub>4</sub>. The promotion of oxidation reactions in the bulk solution as a result  
 253 of the indirect formation of reactive oxygen species, produced by the presence of different inorganic  
 254 ions like SO<sub>4</sub><sup>2-</sup>, Cl<sup>-</sup>, etc, may be the reason behind this finding (Katsaounis and Souentie, 2013;  
 255 Velegraki et al., 2010).

256 Indeed, Dominguez et al. (2016), in their study on parabens BDD oxidation, observed a great  
 257 synergistic effect on the oxidation efficiency in the river water matrix, possibly due to the presence  
 258 of chloride ions at high concentration (40.4 mg/L), which augments the solution conductivity and  
 259 favors the formation of secondary oxidants such as HClO/ClO<sup>-</sup> or chlorine.

260 Regarding the presence of HA, it is well known that HA negatively affects the oxidation process by  
 261 competing with BP for reactive species and electrode surface sites, leading to reduced degradation  
 262 rates (Frontistis et al., 2018; Fernandes et al., 2016b). For example, Woisetschläger et al. (2013)  
 263 noted that glucose degradation became progressively inhibited by increasing the amount of HA.  
 264 Similarly, in the study of Frontistis et al. (2018) on the BDD electrochemical destruction of  
 265 antibiotic ampicillin, the presence of 10 mg/L of HA led to a decrease in the observed kinetic  
 266 constant by 40%. It must be noted here that although HA is typically selected as an analogue of the  
 267 natural organic matter in water matrices, the effluent organic matter in WW may also contain other  
 268 species such as soluble microbial products and traces of non-biodegradable pollutants. In this view,  
 269 the use of HA may not be fully representative of the organic content in WW matrices.

270 Figures 4B and 4C show the effect of the addition of NaCl and NaHCO<sub>3</sub>, respectively, while Figure  
 271 4D shows the effect of the addition of sodium persulfate (SPS) in UW which is a mild oxidant  
 272 (redox potential of 2.1 V) and has the ability to oxidize organic pollutants (Ioannidi et. al., 2018).  
 273 Furthermore, SPS activation causes the production of sulfate radicals with a redox potential of (2.5–  
 274 3.1) V, according to reaction (1), which can be used for the elimination of organic pollutants  
 275 (Matzek and Carter, 2016; Ghanbari et al., 2017).

276

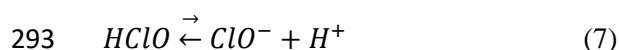
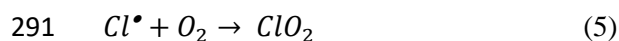
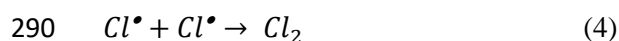
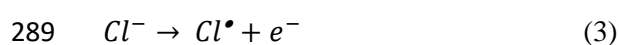
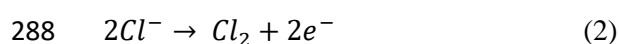


278



279 The presence of bicarbonate anion slightly slows down the rate of oxidation of BP (Figure 4C)  
 280 possibly as a result of the fact that the bicarbonate anion scavenges hydroxyl radicals (Wu and  
 281 Linden, 2010). In contrast, the addition of chloride (Figure 4B) favors the reaction presumably due  
 282 to the formation of chlorine-based oxidative species, including chlorohydroxyl radicals according to  
 283 reactions (2-7). In bibliography, the positive effect of  $Cl^-$  has often been underlined (Garcia-  
 284 Espinoza et al., 2018; Frontistis et al., 2017; Katsaounis and Souentie, 2013). Garcia-Espinoza et al.  
 285 (2018), focused on the effect of electrocatalytically generated active chlorine on carbamazepine  
 286 destruction.

287



294

295 Similar results with the present study were reported by Lebig- Elhadi et al. (2018). They  
 296 investigated the BDD anode oxidation of thiamethoxam with 0.1 M  $Na_2SO_4$  and mentioned that the  
 297 addition of NaCl at concentrations reaching 100 mg/L increased degradation. They also reported  
 298 that the  $k_{app}$  was  $0.72 \text{ min}^{-1}$  at 100 mg/L NaCl and  $0.22 \text{ min}^{-1}$  without NaCl. A similarly positive but  
 299 less pronounced effect was recorded for the addition of 100 and 200 mg/L sodium persulfate  
 300 (Figure 4D). This behavior can be attributed to the electrochemical activation of persulfate for the  
 301 generation of selective sulfate radicals (Frontistis et al., 2018; Chen et al., 2018).

302 Candia-Onfray et al. (2018) showed recently that high concentrations of sulfate and chloride  
 303 support the production of oxidants (e.g. active chlorine species, hydroxyl radicals) that can  
 304 eventually oxidize the organic loading of winery wastewater in the bulk solution. In the work of  
 305 Oliveira et al. (2018) focusing on the electrooxidation of industrial phenolic wastewaters, it was  
 306 shown that the presence of chloride in the wastewater favored the electrogeneration of  
 307 strong oxidant species, (mainly hypochlorous acid, but also chlorine, and hypochlorite) and  
 308 increased the efficiency of the process. The effect of the presence of chloride ion on the oxidation  
 309 process of various synthetic samples was also studied by Fernandes et al. (2016a), who reported that  
 310 the presence of chlorides enhanced the removal of organic matter and nitrogen. The same research  
 311 group (Fernandes et al., 2016b) studied the EO of HA and sanitary landfill leachate samples. It was

312 shown that the conversion of organics and nitrogen increased with the chloride ion concentration,  
313 and the applied current density.

314 However, it should be noted that although electrochemical degradation is usually enhanced by  
315 chloride ions, this is unfortunately accompanied by the formation of undesired organochlorinated  
316 by-products. These products alongside with residual chlorine may both be incriminated for elevated  
317 post-treatment ecotoxicity (Garcia-Segura et al., 2015; Katsoni et al., 2014; Boudreau et al., 2010).  
318 Barazesh et al. (2016) showed that transformation rates for the vast majority of the contaminants in  
319 industrial wastewater increased with chlorides, but high concentrations of  $\text{HCO}_3^-$  frequently altered  
320 transformation rates because of the creation of selective oxidants. Electron-poor contaminants were  
321 found to have a decreased reactivity, while compounds with phenolic and amine moieties were  
322 characterized by increased reactivity. In the same study, it was found that the addition of 10 mM  
323  $\text{HCO}_3^-$  declined the degradation of different pollutants by 50% to 75% relative to the conversion in  
324 10 mM NaCl (Barazesh et al., 2016).

325 Treatment performance may also be affected by effluent pH (Tsantaki et al., 2012), whose effect  
326 hinges on the nature of the implicated organics. Since the various matrices have different pH values  
327 (between 6 and 8), experiments were performed in UW at initial pH values between 3 and 8.  
328 Interestingly, Figure 4E shows no pH effect on degradation of 0.5 mg/L BP. In all cases complete  
329 degradation can be reached within 15 min. Similar results about the slight influence of initial pH on  
330 the oxidation of organic micropollutants using BDD oxidation were reported by Frontistis et. al.  
331 (2017), Pereira et al. (2012) and El-Ghenymy et al. (2012). However, other studies reported  
332 contradictory results concerning the pH effect on the BDD EO (Siedlecka et al., 2018; Abdelhay et  
333 al., 2017; Garcia-Segura et al., 2015). pH was found to have a remarkable role on the removal rate  
334 of BPA, which was favored at pH 10 (Murugananthan et al., 2008). Moreover, the electrochemical  
335 abatement of sulfonamides was strongly affected by pH, alongside other operating conditions such  
336 as temperature and inorganic ions (Fabianska et al., 2014).

337 Finally, representative experiments were performed in the presence of 1000 mg/L t-butanol, whose  
338 affinity for hydroxyl radicals is well-documented (Li et al., 2013). The results are shown in Figure  
339 4F in terms of apparent rate constants in the absence (black bars) and in the presence (dashed bars)  
340 of alcohol. It must be noted here that the latter values have been multiplied 100 times to allow for  
341 clarity. Evidently, the reaction is nearly completely quenched in the presence of alcohol irrespective  
342 of the water matrix, thus implying that hydroxyl radicals are the dominant oxidizing species.

343

#### 344 *3.1.5. Effect of low current in various water matrices*

345 One of the major disadvantages of electrolysis is the need for large amounts of energy. For this  
346 reason, the performance of the process in different aqueous matrices was studied at a lower current

347 density.

348 The effect of low current density (1.4 mA/cm<sup>2</sup>) on 0.5 mg/L BP concentration with 0.1 M Na<sub>2</sub>SO<sub>4</sub>  
 349 and various matrices (WW, WW without the addition of electrolyte, BW, UW and 200 mg/L NaCl  
 350 in UW) is shown in Figure 5; the rate decreases in the order UW with NaCl>WW without  
 351 salt>WW>BW>UW. Concerning WW, BW and UW, it is noticed that the degradation follows the  
 352 same trend as in Figure 4A, but the time needed for the removal of BP is increased. For WW, the  
 353 time required for BP removal was augmented from 3 min at 50 mA/cm<sup>2</sup> to more than 15 min at 1.4  
 354 mA/cm<sup>2</sup>. The addition of 0.1 M Na<sub>2</sub>SO<sub>4</sub> slightly decreased the degradation rate in WW, as can be  
 355 seen in Figure 5. It should be emphasized that the decreased current density does not significantly  
 356 affect the conversion of BP since it becomes 100% and 90% in 5 min at 50 mA/cm<sup>2</sup> and 1.4  
 357 mA/cm<sup>2</sup>, respectively. This result confirms the significance of chloride during BDD anodic  
 358 oxidation as it leads to the formation of active chlorine species (Zhang et al., 2016).

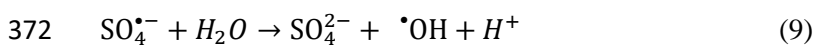
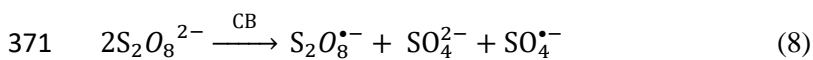
359 Contrarily, the degradation rate of BP in BW and UW was suspended. A possible explanation for  
 360 this result is the strong dependence between current density and the generation of hydroxyl radicals  
 361 that are the principal oxidizing species in the absence of chlorides. As already mentioned, the  
 362 formation of hydroxyl radicals is favored by the augmentation of current density, which in turn may  
 363 maximize the mineralization of organic pollutants.

364

### 365 3.1.6. Comparison with SR-AOPs

366 As already demonstrated in Figure 4D, the presence of SPS can promote the electrochemical  
 367 oxidation of BP due to the formation of sulfate radicals. Since SR-AOPs have recently gained  
 368 attention in water treatment, we decided to compare the EO of BP with that of persulfate oxidation  
 369 activated by carbocatalysis, as follows (Dimitriadou et al., 2019):

370



373

374 The concentration levels of the oxidant and the activator are critical for the efficient degradation of  
 375 BP, as this is demonstrated in Figure 6. The degradation rate increases with increasing either SPS or  
 376 CB concentration within the concentration ranges tested, however the maximum rate recorded in  
 377 either case (Figure 6B and 6D) is lower than that of EO at current densities  $\geq 50$  mA/cm<sup>2</sup> (Figure  
 378 2B). It is also noted that CB behaves as adsorbent since about 35% BP removal occurs after 45 min  
 379 in the absence of SPS (Figure 6A); this is consistent with its considerable specific surface area of  
 380 216 m<sup>2</sup>/g (Dimitriadou et al., 2019). On the other hand, SPS itself is a mild oxidant as 30%  
 381 degradation occurs after 45 min without activator (Figure 6C).

382 The performance of the SR-AOP in actual matrices is demonstrated in Figure 7A; unlike what  
383 happens in EO, degradation efficiency decreases with matrix complexity, i.e. UW>BW>WW. This  
384 also is consistent with the negative impact of bicarbonate (Figure 7B) and chloride (Figure 7D) on  
385 BP degradation. Bicarbonate may scavenge the highly active sulfate and/or hydroxyl radicals  
386 producing the less reactive carbonate radicals ( $HCO_3^{\bullet}$ ) (Ma et al., 2018). On the other hand, sulfate  
387 radicals may react with chloride (Lutze et al., 2015) to form other less reactive radicals such as  
388 chlorine and dichloride radicals ( $Cl^{\bullet}$ ,  $Cl_2^{\bullet-}$ ) (Metheniti et al., 2018), thus lowering degradation rates.  
389 Noticeably, the effect of HA on degradation was found to be commonly detrimental for both EO  
390 (Figure 4A) and SR-AOP (Figure 7C); in the latter case, HA may occupy active sites of the CB  
391 surface, thus limiting availability for SPS and/or BP.

392 To evaluate indirectly the relative contribution of sulfate and hydroxyl radicals to BP degradation,  
393 experiments were conducted with methanol and t-butanol as radical scavengers and the results, in  
394 terms of apparent rate constants, are summarized in Figures 7E and 7F, respectively. Noticeably,  
395 methanol inhibits considerably BP degradation and this is more pronounced at 1000 mg/L  
396 concentration, however, this seems not to be the case with t-butanol. Given that butanol has a 6-fold  
397 greater affinity for hydroxyl radicals than methanol (Li et al., 2013), it can be hypothesized that  
398 sulfate radicals play a key role in degrading BP.

399

#### 400 4. Conclusions

401 This work demonstrates the efficient application of BDD anodic oxidation for the destruction of  
402 butyl paraben, a representative endocrine disrupting compound of the parabens family, in  
403 environmentally relevant matrices and levels. The process is expectedly favored (i) at increased  
404 current densities, where the rate of ROS production is accelerated, and (ii) in the presence (intrinsic  
405 or deliberate) of ions such as chloride that can electrochemically generate additional chlorine-based  
406 oxidative species. As a matter of fact, there appears to be a reaction rate trade-off between high  
407 current densities and chlorine-free electrolytes and vice versa. What is less expected is the fact that  
408 matrix complexity seems to favor paraben degradation. This finding underlines the existence of  
409 some kind of synergy between the organic and/or inorganic water matrix constituents, ROS and the  
410 anode surface. This positive interplay, however, seems to be process-specific as has been  
411 demonstrated through the application of an SR-AOP, where persulfate was carbocatalytically  
412 activated and the resulting sulfate radicals could degrade butyl paraben; in this case, matrix  
413 complexity was detrimental to degradation.

414 Nowadays, an issue of great concern is the design of advanced technologies for the removal or  
415 persistent pollutants from different water matrices. The obtained results showed the water matrix

416 effect on the degradation of BP and underlined the need for further work on the in-depth  
417 examination of the EO of organic compounds and the application of this technology in real life  
418 systems.

419

## 420 **References**

421

422 Abdelhay, A., Jum'h, I., Abdulhay, E., Al-Kazwini, A., Alzubi, M., 2017. Anodic oxidation of  
423 slaughterhouse wastewater on boron-doped diamond: process variables effect. *Water Sci. Technol.*  
424 76(11-12), 3227-3235.

425 Abid, M.F., Alwan, G.M., Abdul-Ridha, L.A., 2016. Study on catalytic wet air oxidation process  
426 for phenol degradation in synthetic wastewater using trickle bed reactor. *Arab. J. Sci. Eng.* 41(7),  
427 2659-2670.

428 Anglada, A., Urriaga, A., Ortiz, I., Mantzavinos, D., Diamadopoulos, E., 2011. Boron-doped  
429 diamond anodic treatment of landfill leachate: evaluation of operating variables and formation of  
430 oxidation by-products. *Water Res.* 45(2), 828–838.

431

432 Barazesh, J.M., Prasse, C., Sedlak, D.L., 2016. Electrochemical transformation of trace organic  
433 contaminants in the presence of halide and carbonate ions. *Environ. Sci. Technol.* 50(18), 10143-  
434 10152.

435

436 Boudreau, J., Bejan, D., Li, S., Bunce, N.J., 2010. Competition between electrochemical advanced  
437 oxidation and electrochemical hypochlorination of sulfametho-xazole at a boron-doped diamond  
438 anode. *Ind. Eng. Chem. Res.* 49, 2537–2542.

439

440 Burgos-Castillo, R.C., Sires, I., Sillanpaa, M., Brillas, E., 2018. Application of electrochemical  
441 advanced oxidation to bisphenol A degradation in water. Effect of sulfate and chloride ions.  
442 *Chemosphere* 194, 812-820.

443

444 Candia-Onfray, C., Espinoza, N., Sabino da Silva, E.B., Toledo-Neira, C., Espinoza,  
445 L.C., Santander, R., García, V., Salazar, R., 2018. Treatment of winery wastewater by  
446 anodic oxidation using BDD electrode. *Chemosphere* 206, 709-717.

447

448 Chen, L., Lei, C., Li, Z., Yang, B., Zhang, X., Lei, L., 2018. Electrochemical activation of sulfate  
449 by BDD anode in basic medium for efficient removal of organic pollutants. *Chemosphere* 210, 516-  
450 523.

451

452 Deligiorgis, A., Xekoukoulotakis, N.P., Diamadopoulos, E., Mantzavinos, D., 2008.  
453 Electrochemical oxidation of table olive processing wastewater over boron-doped diamond  
454 electrodes: Treatment optimization by factorial design. *Water Res.* 42, 1229-1237.

455 Dimitriadou, S., Frontistis, Z., Petala, A., Bampos, G., Mantzavinos, D., 2019. Carbocatalytic  
456 activation of persulfate for the removal of drug diclofenac from aqueous matrices *Catal. Tod.*, in  
457 press

458 Domínguez, J.R., González T., Palo, P., Sánchez-Martín, J., 2010. Electrochemical advanced  
459 oxidation of carbamazepine on boron-doped diamond anodes. Influence of operating variables. *Ind.*  
460 *Eng. Chem. Res.* 49, 8353-8359.

461

- 462 Domínguez, J.R., Muñoz-Peña, M.J., González, T., Palo, P., Cuerda-Correa, E.M., 2016.  
463 Parabens abatement from surface waters by electrochemical advanced oxidation with boron  
464 doped diamond anodes. *Environ. Sci. Pollut. Res. Int.* 23(20), 20315-20330.  
465
- 466 El-Ghenymy, A., Arias, C., Cabot, P.L., Centellas, F., Garrido, J.A., Rodriguez, R.M.,  
467 Brillas, E., 2012. Electrochemical incineration of sulfanilic acid at a boron-doped diamond anode.  
468 *Chemosphere* 87, 1126-1133.  
469
- 470 Fabiańska, A., Białk-Bielińska, A., Stepnowski, P., Stolte, S., Siedlecka, E.M., 2014.  
471 Electrochemical degradation of sulfonamides at BDD electrode: kinetics, reaction pathway and eco-  
472 toxicity evaluation. *J. Hazard. Mater.* 280, 579-587.  
473
- 474 Fernandes, A., Coelho, J., Ciríaco, L., Pacheco, M.J., Lopes, A., 2016a. Electrochemical wastewater  
475 treatment: influence of the type of carbon and of nitrogen on the organic load removal. *Environ.*  
476 *Sci. Pollut. Res. Int.* 23(24), 24614-24623.  
477
- 478 Fernandes, A., Santos, D., Pacheco, M.J., Ciríaco, L., Lopes, A., 2016b.  
479 Electrochemical oxidation of humic acid and sanitary landfill leachate: Influence of anode material,  
480 chloride concentration and current density. *Sci. Total Environ.* 541, 282-291.  
481
- 482 Fransway, A.F., Fransway, P.J., Belsito, D.V., Warshaw, E.M., Sasseville, D., Fowler, J.F.  
483 Jr., DeKoven, J.G., Pratt, M.D., Maibach, H.I., Taylor, J.S., Marks, J.G., Mathias, C.G.T., DeLeo,  
484 V.A., Zirwas, J.M., Zug, K.A., Atwater, A.R., Silverberg, J., Reeder, M.J., 2019a. Parabens.  
485 *Dermatitis* 30, 3-31.  
486
- 487 Fransway, A.F., Fransway, P.J., Belsito, D.V., , Yiannias, J.A., 2019b. Paraben toxicology.  
488 *Dermatitis* 30, 32-45.  
489
- 490 Frontistis, Z., Mantzavinos, D., 2017. *Wastewater and Biosolids Management*, IWA Publishing,  
491 132.  
492
- 493 Frontistis, Z., Mantzavinos, D., Meriç, S., 2018. Degradation of antibiotic ampicillin on boron-  
494 doped diamond anode using the combined electrochemical oxidation - Sodium persulfate process. *J.*  
495 *Environ. Manage.* 223, 878-887.  
496
- 497 Frontistis, Z., Antonopoulou, M., Yazirdagi, M., Kilinc, Z., Konstantinou, I., Katsaounis,  
498 A., Mantzavinos, D., 2017. Boron doped diamond electrooxidation of ethyl paraben:  
499 The effect of electrolyte on by-products distribution and mechanisms. *J. Environ. Manage.* 195(Pt  
500 2), 148-156.  
501
- 502 García-Espinoza, J.D., Mijaylova-Nacheva, P., Avilés-Flores, M, 2018. Electrochemical  
503 carbamazepine degradation: Effect of the generated active chlorine, transformation pathways and  
504 toxicity. *Chemosphere* 192, 142-151.  
505
- 506 Garcia-Segura, S., Keller, J., Brillas, E., Radjenovic, J.,  
507 2015. Removal of organic contaminants from secondary effluent by anodic oxidation with a boron-  
508 doped diamond anode as tertiary treatment. *J. Hazard. Mater.* 283, 551-557.  
509
- 510 Ghanbari, F., Moradi M., 2017. Application of peroxymonosulfate and its activation methods for  
511 degradation of environmental organic pollutants: review, *Chem. Eng. J.* 310, 41-62.  
512

- 513 Giger, W., Gabriel, F., Jonkers, N., Wettstein, F., Kohler, H., 2009. Environmental fate of phenolic  
514 endocrine disruptors: field and laboratory studies. *Philosophical Transactions of the Royal Society*  
515 *A: Mathematical. Phys. Eng. Sci.* 367(1904), 3941–3963.  
516
- 517 Gomes, F.E.R., de Souza, N.E., Galinaro, Carlos A., Arriveti, L.O.R., de Assis, J.B., Tremiliosi-  
518 Filho, G., 2016. Electrochemical degradation of butyl paraben on platinum and glassy carbon  
519 electrodes. *J. Electroanal. Chem.* 769, 124-130.  
520
- 521 Guinea, E., Arias, C., Cabot, P.L., Garrido, J.A., Rodríguez, R.M., Centellas, F., Brillas, E., 2008.  
522 Mineralization of salicylic acid in acidic aqueous medium by electrochemical advanced oxidation  
523 processes using platinum and boron-doped diamond as anode and cathodically generated hydrogen  
524 peroxide. *Water Res.* 42, 499–511.  
525
- 526 Haman, C., Dauchy, X., Rosin, C., Munoz, J.F., 2015. Occurrence, fate and behavior of parabens in  
527 aquatic environments: a review. *Water Res.* 68, 1-11.  
528
- 529 Henke, A.H., Saunders, T.P., Pedersen, J.A., Hamers, R.J., 2019.  
530 Enhancing electrochemical efficiency of hydroxyl radical formation on diamond electrodes by  
531 functionalization with hydrophobic monolayers. *Langmuir* 35(6), 2153-2163.  
532
- 533 Ioannidi, A., Frontistis, Z., Mantzavinos, D., 2018. Destruction of propyl paraben by persulfate  
534 activated with UV-A light emitting diodes. *Journal of Environ. Chem. Eng.* 6, 2992–2997.  
535
- 536 Katsoni, A., Mantzavinos, D., Diamadopoulou, E., 2014. Coupling digestion in a pilot-scale UASB  
537 reactor and electrochemical oxidation over BDD anode to treat diluted cheese whey. *Environ. Sci.*  
538 *Pollut. Res. Int.* 21(21), 12170-12181.  
539
- 540 Katsaounis, A., Souentie, S., 2013. In: Savinell, R.F., Ota, Ken-ichiro, Kreysa, G. (Eds.), *In-cell*  
541 *Mediated (Via Active Chlorine) Electrochemical Oxidation of Organic*.  
542
- 543 Kenova, T.A., Kornienko, G.V., Golubtsova, O.A., Kornienko, V.L., Maksimov, N.G., 2018.  
544 Electrochemical degradation of Mordant Blue 13 azo dye using boron-doped diamond and  
545 dimensionally stable anodes: influence of experimental parameters and water matrix. *Environ. Sci.*  
546 *Pollut. Res. Int.* 25(30), 30425-30440.  
547
- 548 Klavarioti, M., Mantzavinos, D., Kassinos, D., 2009. Removal of residual pharmaceuticals from  
549 aqueous systems by advanced oxidation processes. *Environ. Int.* 35(2), 402-417.  
550
- 551 Kouskouki, A., Chatzisyneon, E., Mantzavinos, D., Frontistis, Z., 2019. Electrochemical  
552 Degradation of Piroxicam on a Boron-Doped Diamond Anode: Investigation of Operating  
553 Parameters and Ultrasound Synergy. *ChemElectroChem* 6, 841-847.  
554
- 555 Kraft, A., Stadelmann, M., Blaschke, M., 2003. Anodic oxidation with doped diamond electrodes: a  
556 new advanced oxidation process. *J. Hazard. Mater.* 103(3), 247-261.  
557
- 558 Lebig-Elhadi, H., Frontistis, Z., Ait-Amar, H., Amrani, S., Mantzavinos, D., 2018. Electrochemical  
559 oxidation of pesticide thiamethoxam on boron doped diamond anode: Role of operating parameters  
560 and matrix effect. *Process Saf. Environ.* 116, 535-541.  
561

- 562 Li, B., Li, L., Lin, K., Zhang, W., Lu, S., Luo, Q., 2013. Removal of 1,1,1-trichloroethane from  
563 aqueous solution by a sono-activated persulfate process. *Ultrason. Sonochem.* 20, 855-863.
- 564
- 565 Liao, C., Liu, F., Kannan, K., 2013. Occurrence of and dietary exposure to parabens in foodstuffs  
566 from the United States. *Environ. Sci. Technol.* 47, 3918-3925.
- 567
- 568 Lounasvuori, M.M., Kelly, D., Foord, J.S., 2018. Carbon black as low-cost alternative for  
569 electrochemical sensing of phenolic compounds. *Carbon* 129, 252-257.
- 570
- 571 Lutze, H.V., Kerlin, N., Schmidt, T.C., 2015. Sulfate radical-based water treatment in presence of  
572 chloride: Formation of chlorate, inter-conversion of sulfate radicals into hydroxyl radicals and  
573 influence of bicarbonate. *Water Res.* 72, 349-360.
- 574
- 575 Ma, J., Li, H., Yang, Y., Li, X., 2018. Influence of water matrix species on persulfate oxidation of  
576 phenol: reaction kinetics and formation of undesired degradation byproducts. *Water Sci. Technol.*  
577 2017, 340-350.
- 578
- 579 Matzek, L.W., Carter, K. E., 2016. Activated persulfate for organic chemical degradation: a review.  
580 *Chemosphere* 151, 178-188.
- 581
- 582 Metheniti, M.E., Frontistis, Z., Ribeiro, R.S., Silva, A.M.T., Faria, J.L., Gomes, H.T., Mantzavinos,  
583 D., 2018. Degradation of propyl-paraben by activated persulfate using iron-containing magnetic  
584 carbon xerogels: investigation of water matrix and process synergy effects, *Environ. Sci. Pollut.*  
585 *Res.* 25, 34801-34810.
- 586
- 587 Murugananthan, M., Yoshihara, S., Rakuma, T., Shirakashi, T., 2008.  
588 Mineralization of bisphenol A (BPA) by anodic oxidation with boron-  
589 doped diamond (BDD) electrode. *J. Hazard. Mater.* 154(1-3), 213-220.
- 590
- 591 Oliveira, E.M.S., Silva, F.R., Morais, C.C.O., Oliveira, T.M.B.F., Martínez-Huitle, C.A., Motheo,  
592 A.J., Albuquerque, C.C., Castro, S.S.L., 2018. Performance of (in)active anodic materials for the  
593 electrooxidation of phenolic wastewaters from cashew-nut processing industry.  
594 *Chemosphere* 201,740-748.
- 595
- 596 Pecková, K., Musilová, J., Barek, J., 2009. Boron-doped diamond film electrodes—new tool for  
597 voltammetric determination of organic substances. *Crit. Rev. Anal. Chem.* 39:3, 148-172.
- 598
- 599 Pereira, G.F., Rocha-Filho, R.C., Bocchi, N., Biaggio, S.R., 2012. Electrochemical degradation of  
600 bisphenol A using a flow reactor with a boron-doped diamond anode. *Chem. Eng. J.* 198-199, 282-  
601 288.
- 602
- 603 Reeder, M., Atwater, A.R., 2019. Parabens: the 2019 nonallergen of the year. *Cutis.* 103(4), 192-  
604 193.
- 605
- 606 Sarkka, H., Bhatnagar, A., Sillanpaa., M., 2015. Recent developments of electro-oxidation in water  
607 treatment – a review. *J. Electroanal. Chem.* 754, 46-56.
- 608
- 609 Siedlecka, E.M., Ofiarska, A., Borzyszkowska, A.F., Białk-Bielińska, A., Stepnowski,  
610 P., Pieczyńska, A., 2018. Cytostatic drug removal using  
611 electrochemical oxidation with BDD electrode: Degradation pathway and toxicity. *Water Res.* 144,  
612 235-245.



- 613  
614 Steter, J.R., Rocha, R.S., Dionisio, D., Lanza, M.R.V., Motheo, A.J., 2014a. Electrochemical  
615 oxidation route of methyl paraben on a boron-doped diamond anode. *Electrochim. Acta* 117, 127-  
616 133.
- 617  
618 Steter, J.R., Dionisio, D., Lanza, M.R.V., Motheo, A.J., 2014b. Electrochemical and  
619 sonoelectrochemical processes applied to the degradation of the endocrine disruptor methyl  
620 paraben. *J. Appl. Electrochem.* 44, 1317-1325.
- 621  
622 Tsantaki, E., Velegraki, T., Katsaounis, A., Mantzavinos, D., 2012.  
623 Anodic oxidation of textile dyehouse effluents on boron-doped diamond electrode. *J. Hazard.*  
624 *Mater.* 207-208, 91-6.
- 625  
626 Tsiampalis, A., Frontistis, Z., Binas, V., Kiriakidis, G., Mantzavinos, D., 2019. Degradation of  
627 Sulfamethoxazole Using Iron-Doped Titania and Simulated Solar Radiation. *Catalysts* 9(7), 612
- 628  
629 Velegraki, T., Balayiannis, G., Diamadopoulos, E., Katsaounis, A., Mantzavinos, D., 2010.  
630 Electrochemical oxidation of benzoic acid in water over boron-doped diamond electrodes: statistical  
631 analysis of key operating parameters, kinetic modeling, reaction by-products and ecotoxicity.  
632 *Chem. Eng. J.* 160, 538-548.
- 633  
634 Woisetschläger, D., Humpl, B., Koncar, M., Siebenhofer, M., 2013. Electrochemical oxidation of  
635 wastewater—opportunities and drawbacks. *Water Sci. Technol.* 65, 1173-1179.
- 636  
637 Wu, C., Linden, K.G., 2010. Phototransformation of selected organophosphorus pesticides: roles of  
638 hydroxyl and carbonate radicals. *Water Res.* 44, 3585-3594.
- 639  
640 Zhang, C., Du, X., Zhang, Z., Fu, D., 2016. The peculiar roles of chloride electrolytes in BDD  
641 anode cells. *RSC Advances* 6, 65638-65643.

## List of Figures

**Figure 1.** Degradation of 0.5 mg/L BP at 50 mA/cm<sup>2</sup> current density with 0.1 M Na<sub>2</sub>SO<sub>4</sub> in UW as a function of anodic material.

**Figure 2.** Effect of current density (in mA/cm<sup>2</sup>) on 0.5 mg/L BP degradation in UW with 0.1 M Na<sub>2</sub>SO<sub>4</sub>. (A) Concentration-time profiles; (B) Apparent rate constants.

**Figure 3.** Effect of BP concentration (in mg/L) on its degradation at 50 mA/cm<sup>2</sup> current density in UW with 0.1 M Na<sub>2</sub>SO<sub>4</sub>. Numbers next to profiles show apparent rate constants (in 1/min)

**Figure 4.** Degradation of 0.5 mg/L BP at 50 mA/cm<sup>2</sup> current density with 0.1 M Na<sub>2</sub>SO<sub>4</sub>. (A) Various actual water matrices and UW spiked with 10 mg/L HA; (B) Addition of chloride (in mg/L ) in UW; (C) Addition of bicarbonate (in mg/L ) in UW; (D) Addition of sodium persulfate (in mg/L ) in UW; (E) Various initial pH values of UW. (F) Apparent rate constants for runs without (black bars) and with (dashed bars) 1000 mg/L tert-butanol. Values for runs with butanol have been multiplied by a factor of 100 for clarity.

**Figure 5.** Effect of low current density (1.4 mA/cm<sup>2</sup>) on 0.5 mg/L BP concentration with 0.1 M Na<sub>2</sub>SO<sub>4</sub> and various matrices. Dashed line shows experiment without addition of electrolyte.

**Figure 6.** Degradation of 0.5 mg/L BP in UW as a function of SPS ((A) and (B)) or CB ((C) and (D)) concentration. For (A) and (B), CB=25 mg/L; for (C) and (D), SPS=250 mg/L.

**Figure 7.** Effect of (A) actual water matrix or UW spiked with (B) bicarbonate; (C) humic acid; (D) chloride; (E) methanol; (F) t-butanol on the degradation of 0.5 mg/L BP with 250 mg/L SPS and 25 mg/L CB. All concentrations in (B)-(F) are in mg/L.

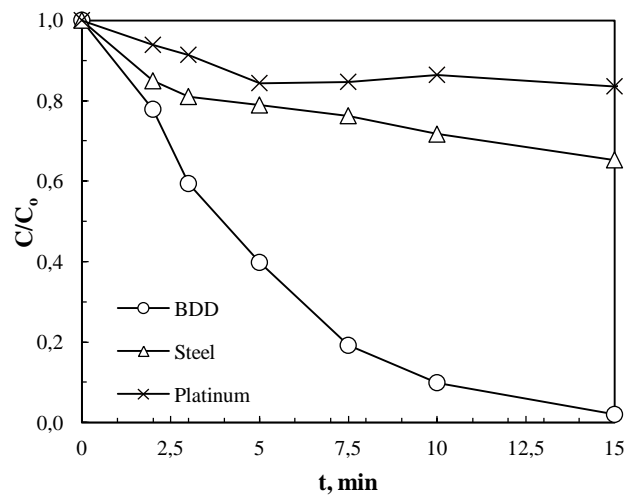


**Figure 1.** Degradation of 0.5 mg/L BP at 50 mA/cm<sup>2</sup> current density with 0.1 M Na<sub>2</sub>SO<sub>4</sub> in UW as a function of anodic material.

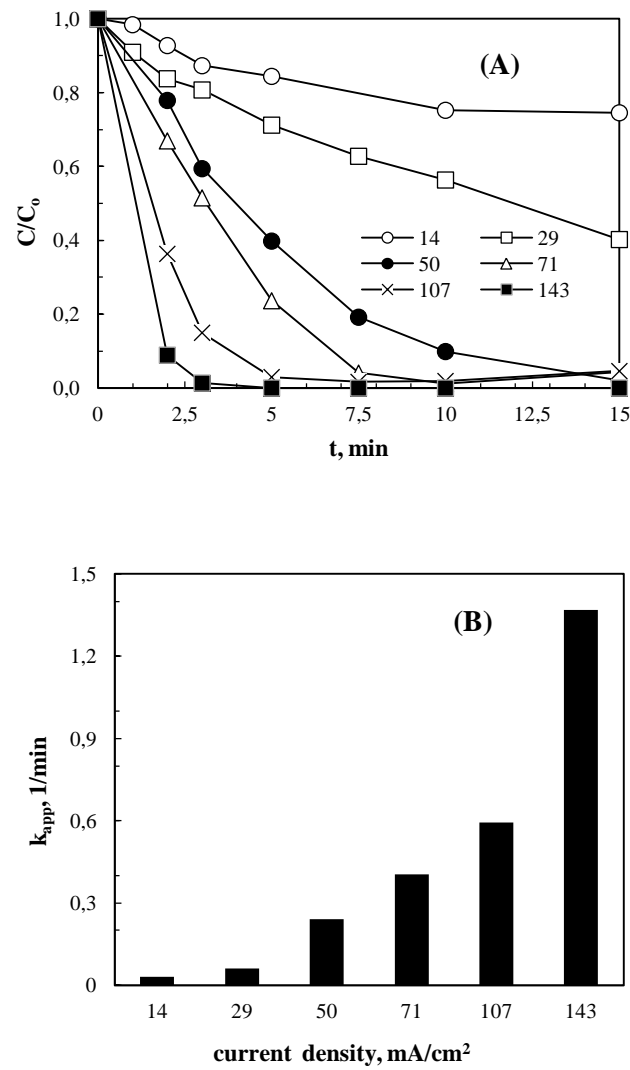


**Figure 2.** Effect of current density (in mA/cm<sup>2</sup>) on 0.5 mg/L BP degradation in UW with 0.1 M Na<sub>2</sub>SO<sub>4</sub>. (A) Concentration-time profiles; (B) Apparent rate constants.

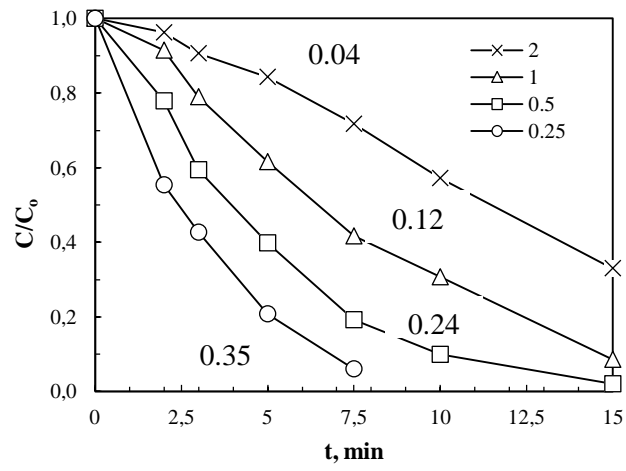


**Figure 3.** Effect of BP concentration (in mg/L) on its degradation at 50 mA/cm<sup>2</sup> current density in UW with 0.1 M Na<sub>2</sub>SO<sub>4</sub>. Numbers next to profiles show apparent rate constants (in 1/min).

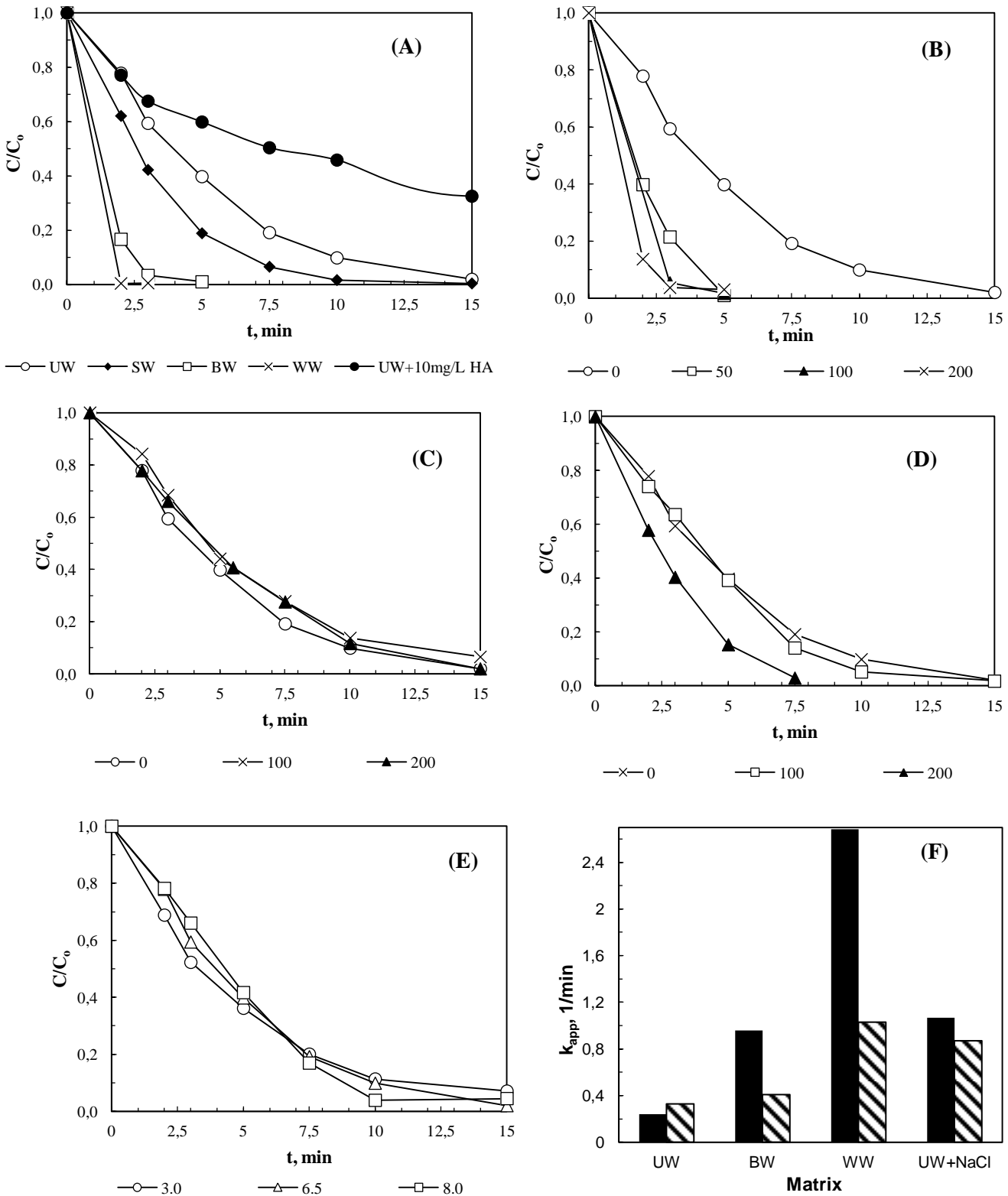


**Figure 4.** Degradation of 0.5 mg/L BP at 50 mA/cm<sup>2</sup> current density with 0.1 M Na<sub>2</sub>SO<sub>4</sub>. (A) Various actual water matrices and UW spiked with 10 mg/L HA; (B) Addition of chloride (in mg/L ) in UW; (C) Addition of bicarbonate (in mg/L ) in UW; (D) Addition of sodium persulfate (in mg/L ) in UW; (E) Various initial pH values of UW. (F) Apparent rate constants for runs without (black bars) and with (dashed bars) 1000 mg/L tert-butanol. Values for runs with butanol have been multiplied by a factor of 100 for clarity.

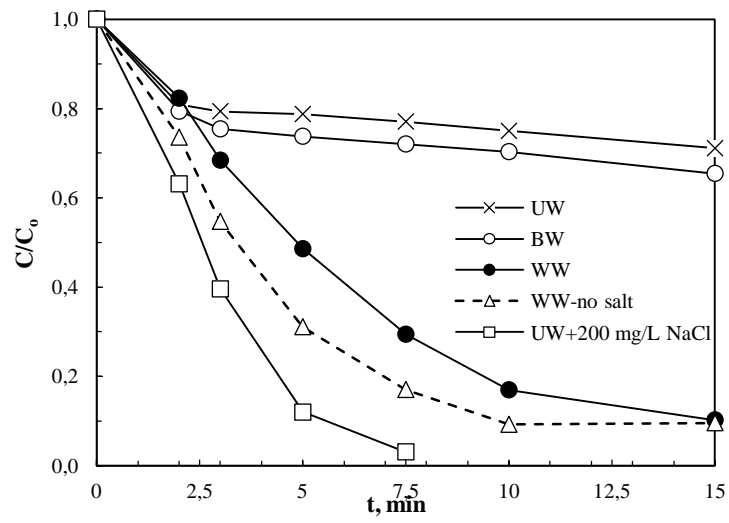


**Figure 5.** Effect of low current density ( $1.4 \text{ mA/cm}^2$ ) on  $0.5 \text{ mg/L}$  BP concentration with  $0.1 \text{ M}$   $\text{Na}_2\text{SO}_4$  and various matrices. Dashed line shows experiment without addition of electrolyte.

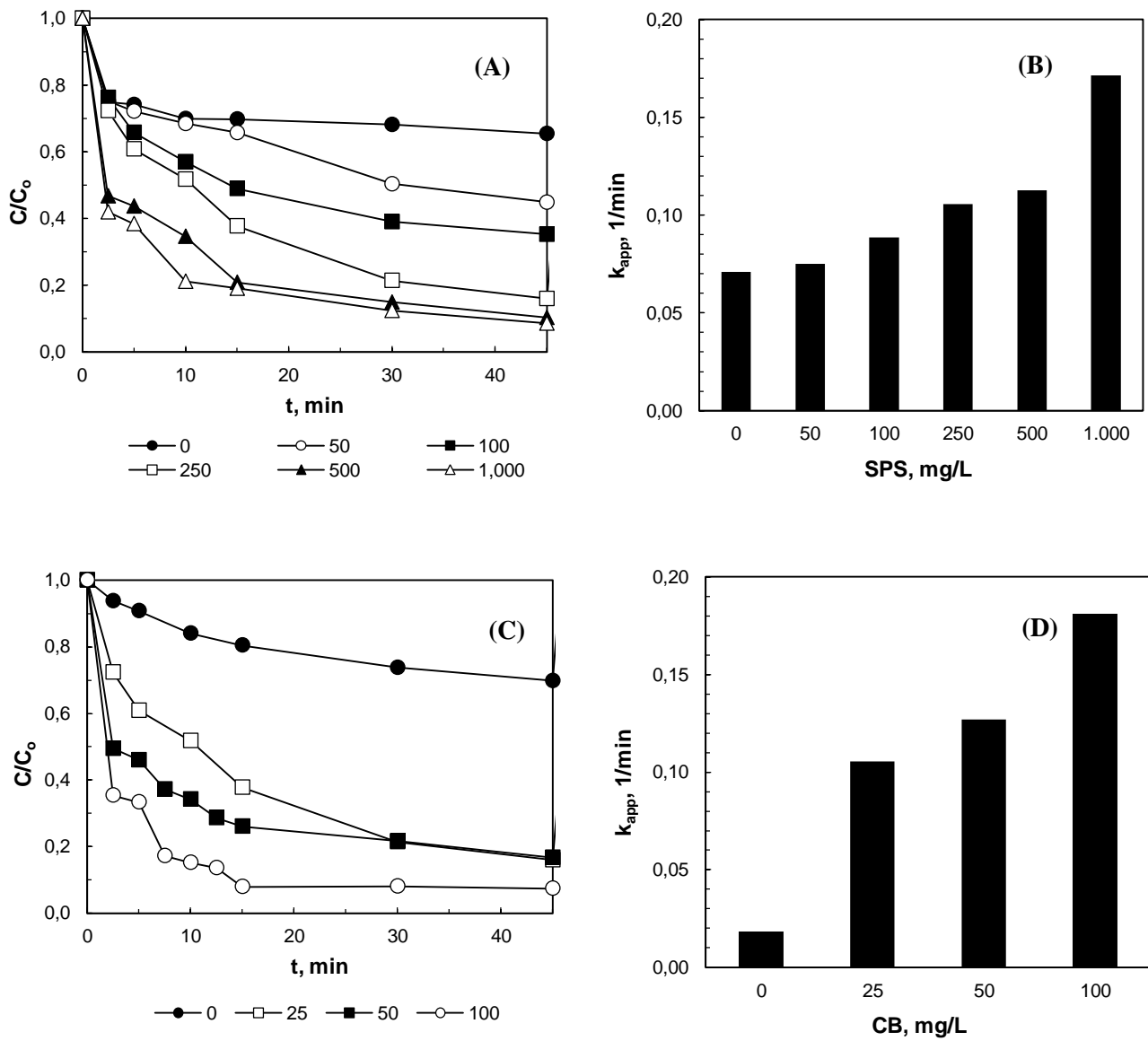


**Figure 6.** Degradation of 0.5 mg/L BP in UW as a function of SPS ((A) and (B)) or CB ((C) and (D)) concentration. For (A) and (B), CB=25 mg/L; for (C) and (D), SPS=250 mg/L.



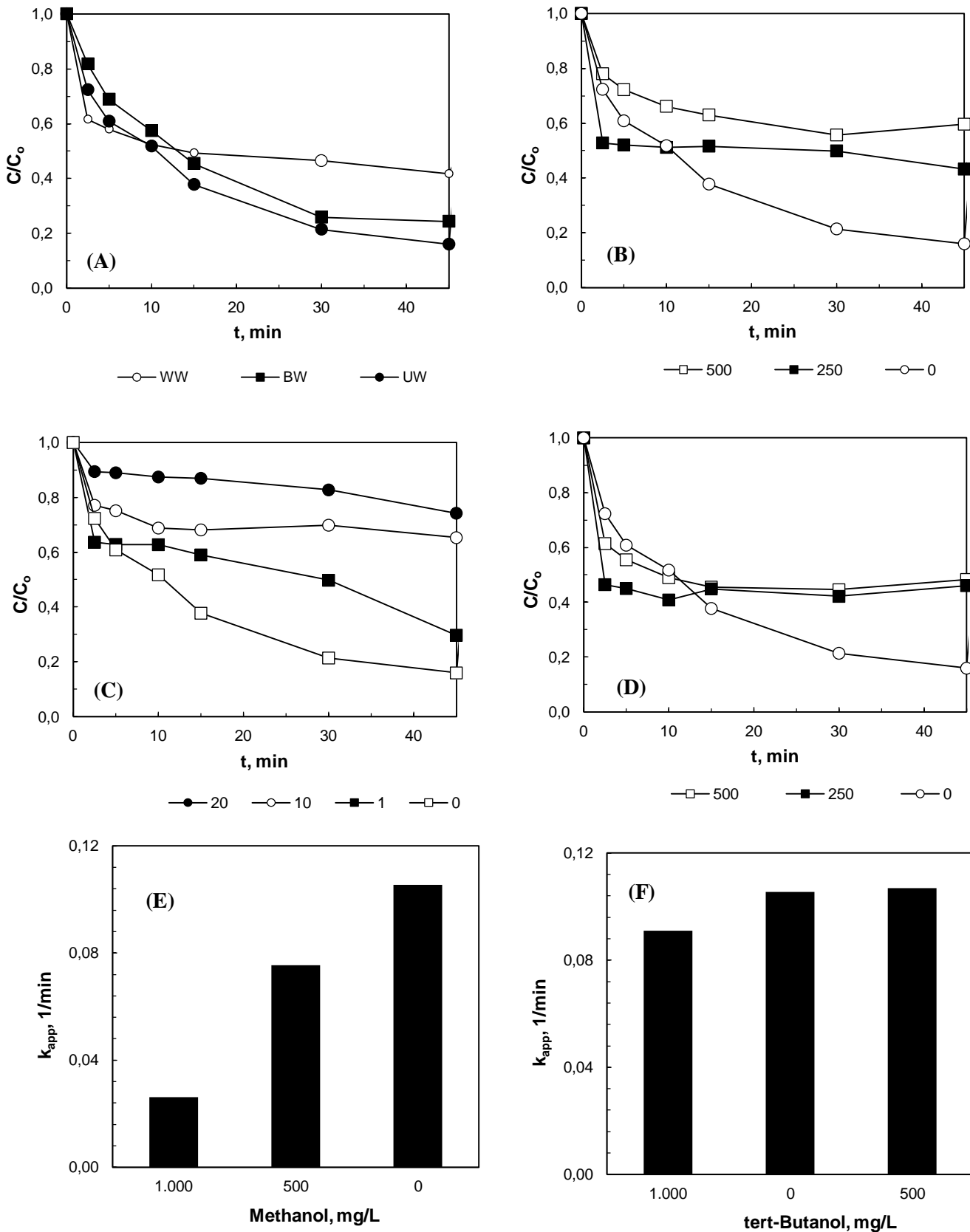


**Figure 7.** Effect of (A) actual water matrix or UW spiked with (B) bicarbonate; (C) humic acid; (D) chloride; (E) methanol; (F) t-butanol on the degradation of 0.5 mg/L BP with 250 mg/L SPS and 25 mg/L CB. All concentrations in (B)-(F) are in mg/L.